

# MICROPHONICS TESTING OF LCLS II CRYOMODULES AT JLAB\*

T. Powers<sup>†</sup>, K. Davis, and N. Brock

Thomas Jefferson National Accelerator Facility, Newport News, VA 23606 USA

## Abstract

Jefferson Lab is partnering with Fermilab to build 40 cryomodules for the LCLS II accelerator that will be installed at the Stanford Linear Accelerator (SLAC). The LCLS II cryomodule is an 8-seat CW cryomodule which operates at 1300 MHz and is based on the XFEL design. The cavities have design loaded-Q of  $4 \times 10^7$ , which means that it has a control bandwidth of 16 Hz. The JLab prototype cryomodule was instrumented with a series of 10 accelerometers, and impulse hammer response measurements were made while the cryomodule was being built and after it was installed in the JLAB cryomodule test facility. This was done so that we could better understand the shapes of the modes of the structure. These results were compared to impulse hammer testing from the outside of the cryomodule to individual cavity frequency shifts when the cryomodule was cold. Additionally, background microphonics and transfer function measurements were made on several other LCLS II cryomodules in the JLab cryomodule test facility (CMTF). The prototype cryomodule had excessive microphonics up to 100 Hz peak due to a thermo-acoustic oscillation in the cryogenic supply circuit. Design modifications were implemented and subsequently the cryomodules had microphonics on the order of 10 to 20 Hz.

## BACKGROUND

Modal measurements, extensive microphonics measurements and impulse hammer to cavity frequency shift measurements were made on the prototype cryomodule. JLAB cryomodules CM03 and CM10 also had impulse hammer testing to frequency shift measurements made and varying amounts of background microphonics measurements were made of six of the 8 cryomodules that have been tested to date.

## Modal Analysis

The modal analysis was done using the standard approach of striking the structure with a force instrumented hammer and measuring either the response of tri-axial accelerometers or changes in the resonant frequency of the cavity. The frequency shift was recorded by using one of the analog outputs of the low level RF chassis while it was operating in a frequency tracking mode known as self-excited loop (SEL) or by recording the phase difference between the field probe and forward power when the systems were operated in a fixed frequency mode known as the generator driven resonator mode (GDR). In general the transfer function is defined as:

$$H(\omega) = \frac{\overline{Y(\omega)}}{\overline{X(\omega)}} \quad (1)$$

Here  $H(\omega)$  is the transfer function which is a complex number in the frequency domain,  $\overline{Y(\omega)}$  is the average of several frequency domain measurements of the system response, accelerometer or cavity frequency shift, and  $\overline{X(\omega)}$  is the average of several corresponding frequency domain measurements of the output of the force sensor. In order to reduce the measurement noise, equation (2) is used for calculating the system response. Here  $X^*(\omega)$  is the complex conjugate of output of the force sensor in the frequency domain.

$$H(\omega) = \frac{\overline{Y(\omega)X^*(\omega)}}{\overline{X(\omega)X^*(\omega)}} \quad (2)$$

## Frequency Shift Measurements

Two methods are used for determining the frequency shift of the cavity. The first method made use of a frequency tracking RF source to excite the cavity. The RF frequency of the output of the field probe port on the cavity was the same frequency as the cavity. This signal is acquired using a digital I/Q receiver where the RF frequency was within 100 Hz of the cavity frequency. The I/Q outputs of the receiver are processed using the following equation:

$$\Delta f = \frac{Q(t) \frac{dI(t)}{dt} - I(t) \frac{dQ(t)}{dt}}{2\pi(I^2(t) + Q^2(t))} \quad (3)$$

Which for a sampled system can be estimated as:

$$\Delta f_i = \frac{Q_i(I_i - I_{i-1}) - I_i(Q_i - Q_{i-1})}{2\pi\Delta t(I_i^2 + Q_i^2)} \quad (4)$$

While both analog [1] and digital methods [2, 3] can be used to process the results, a digital approach was used for this work.

In the second method the cavities are operated with a fixed frequency system which regulates gradient and phase of the cavity where the cavity voltage is given by the following equations:

$$\vec{V}_{RF} \propto \vec{V}_{FP} [1 + j \tan(\varphi_{RF} - \varphi_{OFFSET})] \quad (5)$$

$$\vec{V}_{RF} \propto \vec{V}_{FP} \left( 1 + j \frac{2Q_L \delta f}{f_0} \right) \quad (6)$$

$$\delta f = \frac{f_0}{2Q_L} \tan(\varphi_{RF} - \varphi_{OFFSET}) \quad (7)$$

Here  $\vec{V}_{RF}$  and  $\vec{V}_{FP}$  are the voltage of the RF source and that measured at the field probe port respectively,  $Q_L$  is the loaded-Q of the cavity,  $f_0$  is the center frequency of the

\* Authored by Jefferson Science Associates, LLC under U.S. DOE Contract No. DE-AC05-06OR23177

<sup>†</sup> powers@jlab.org

Content from this work may be used under the terms of the CC BY 3.0 licence (© 2019). Any distribution of this work must maintain attribution to the author(s), title of the work, publisher, and DOI.

cavity,  $\varphi_{RF}$  is the phase of  $\overline{V_{RF}}$  and  $\varphi_{OFFSET}$  is a constant phase offset that is set such that the difference between it and  $\varphi_{RF}$  is zero when the resonant frequency of the cavity is same as that of the RF source.

### RF Power Limitations

The LCLS II system was designed to operate at a gradient of 16 MV/m, a loaded-Q of  $4.12 \times 10^7$  and a maximum beam current of 100  $\mu$ A. The RF sources which have been purchased for the project are designed to deliver 3.8 kW CW. Assuming 5% losses for the transmission lines, circulators, etc. means that the cavities operate with a maximum of 3.6 kW of RF power at the cavity. Figure 1 is a plot of the required RF power and phase for no beam current and for full beam current. It shows that for no or minimal beam loading, the cavities can operate with only 18 Hz of microphonics. When the machine is operated at full beam current, the maximum microphonics before the RF power limitation is met is about 13 Hz.

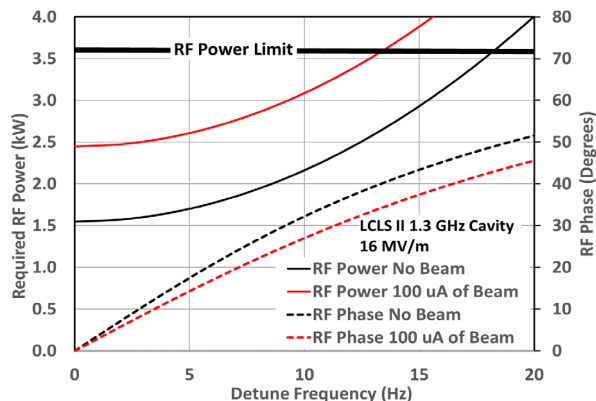


Figure 1: Peak RF power and phase requirements for an LCLS II cavity, as a function of cavity detune frequency for no beam and design beam current.

## RESULTS

Modal measurements were done on the prototype cryomodule at various phases of the fabrication process. Accelerometers were placed on the beam lines between the cavities, where they remained functional until the cryomodule was first cooled down to 2 K at which time, as expected, they failed. This was done as part of the program to better understand the vibrational modes which contribute to microphonics. We also made transfer function measurements from an impulse hammer striking different locations on the outside of the cryomodule to cavity frequency shifts. Background microphonics under several different operating conditions were also measured and analysed.

### Modal and Transfer Function Measurements

Modal measurements were made on the prototype cryomodule string using 10 accelerometers which were placed on the beam line between each cavity as well as on the gate valve at the cavity 1 end of the cryomodule and on

the quadrupole magnet located at the cavity 8 end of the cryomodule. Single-point excitation, multi-point response impulse response testing was done after the string was assembled and prior to insertion into the insulating vacuum vessel. The accelerometers were left in place, connected through vacuum feedthroughs, and the impulse testing was repeated while it was in the cryomodule test facility prior to cool down.

Modal analysis software called MEScope® was used to analyse the resultant transfer functions and to generate animations of the motion of the structure at the accelerometer locations. These results were used to better understand the modes. Further, the animations can be used to identify locations for potential mitigations. Although we did not do so in this instance, the results of this analysis can also be used to validate finite element models of the system. In addition to providing animations the software did a modal analysis and identified 33 significant modes between 3 and 95 Hz. One thing of note is that there is a theoretical shift upward in frequency of about 10% due to the increased stiffness of the structure at cryogenic temperatures. This shift was confirmed in other cryomodules [4].

Transfer function measurements from an impulse hammer strike to cavity frequency shift were taken for three different cryomodules. On two they were done one cavity at a time using a low power RF system which provided about 100 mW to the fundamental power coupler. In these two cases the data for each cryomodule was combined to provide sets of single-excitation multi-response transfer function measurements. In CM10 a remote controlled impulse hammer was used to strike the beamline flange, and in a separate test, the coupler vacuum pipe. Both were done while the cavities were operated using the high power solid state amplifiers. In these cases the detune phase shift data for 7 of the cavities was taken simultaneously with the force sensor signal. Two sets of data were taken and the results from the eighth cavity was combined with the data from the other set to provide a complete transfer function measurement. The results from these measurements are shown in Fig. 2 through 6.

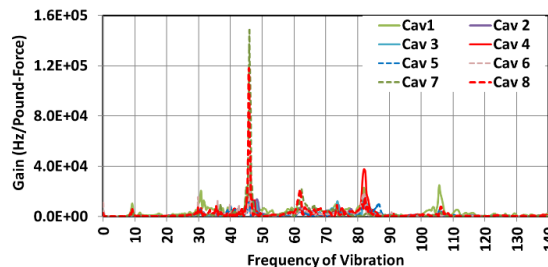


Figure 2: Impulse hammer to delta-F response function for the prototype cryomodule.

Figure 2 shows the results of the impulse hammer tests of the prototype cryomodule where the impact point was the flange on the beam pipe at the cavity 8 end of the cryomodule. The dominant modes which affect the cavity frequencies in this cryomodule from this excitation point are at 46 Hz, 84 Hz, 31 Hz 62 Hz and 100 Hz. As shown in

Fig. 3, there are also vibrational modes which affect the cavity frequencies with at least 20 frequencies between 25 and 95 Hz.

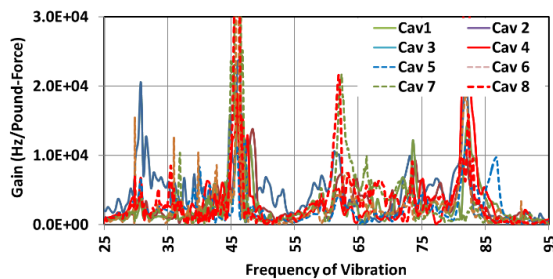


Figure 3: Example of the large number of the modes between 25 Hz and 95 Hz in the prototype cryomodule.

Figures 4 and 5 show the results of impact response tests using the same excitation point for cryomodules CM03 and CM10 respectively. Both of these cryomodules also have the same dominate 46 Hz mode. The difference being that in CM3 it was strongest only in cavity 8 while in CM10 it was strongest in cavities 3, 4, and 5. Review of the modal data taken on the cryomodule string indicate that a likely source of this mode is a vertical vibration of the quadrupole magnet located at the cavity 8 end of the cryomodule.

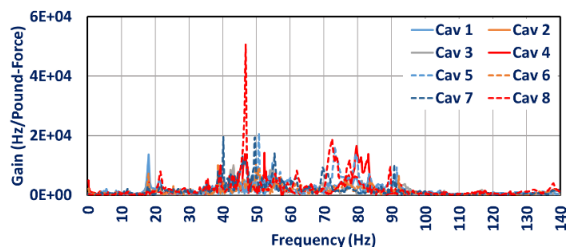


Figure 4: Impulse hammer to delta-F response function for the cryomodule CM03, excitation point was beam pipe at cavity 8 end.

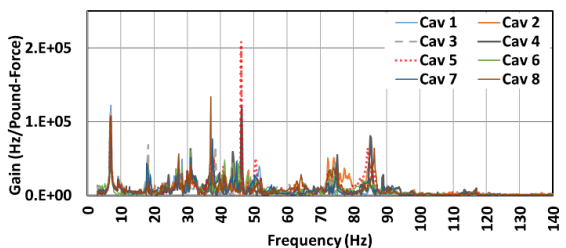


Figure 5: Impulse hammer to delta-F response function for the cryomodule CM10, excitation point was beam pipe at cavity 8 end.

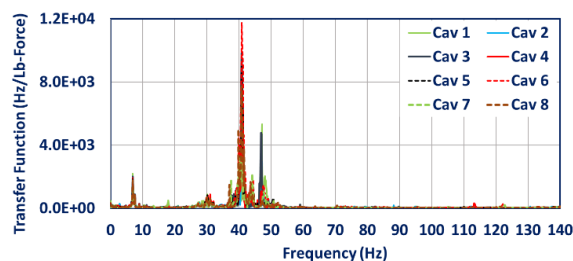


Figure 6: Impulse hammer to delta-F response function for CM10, excitation point was the coupler vacuum manifold.

Figure 6 shows the transfer function from a strike on the coupler vacuum manifold pipe to the 8 cavities in CM10. The vacuum manifold pipe is a vacuum pipe approximately 12 cm in diameter which runs the length of the cryomodule. It connects to each of the RF couplers via a vacuum bellows. Modal measurements and analysis of the vacuum pipe using an impulse hammer and accelerometers indicated that the 41-42 Hz mode is the cavity 1 end of the pipe vibrating mostly horizontally while the cavity 8 end of the pipe is vibrating mostly vertically. This 41 Hz mode is an example of a mode which was not excited by striking the beam line at the cavity 8 end of the cryomodule.

### Background microphonics Measurements

For the prototype cryomodule, the cavities were measured one at a time in SEL mode. This cryomodule suffered from thermoacoustic oscillations (TAO) in the JT valve which was addressed with a design change [5]. JLab staff found an approach to operating our specific installation such that the effects of the TAO were minimized. This involved regulating the liquid level with a valve in an upstream heat exchanger. We designated this mode as the “quiet” state. Figure 7 shows the microphonics for cavity 7 when the cryogenics system was operated in the quiet state. Similar results were obtained with all of the other cavities with the highest “quiet state” microphonics being on cavity 1 at 8 Hz peak. The vibrations at 29.9 Hz and 89.8 Hz are probably due to a nearby motor with a rotational frequency of 1800 rpm. At +/- 8 Hz peak microphonics the system was operating below the target maximum of +/- 10 Hz.

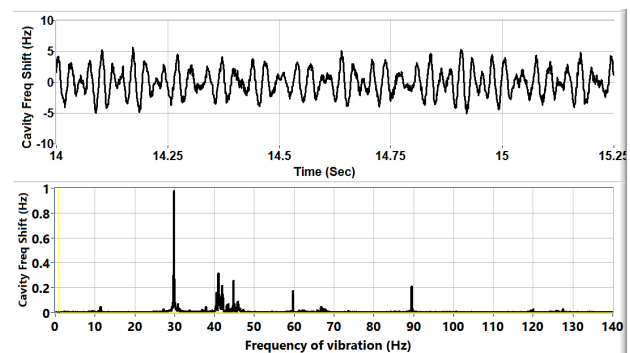


Figure 7: Prototype cryomodule cavity 7 background microphonics when the cryogenics were operated in a quiet state. Upper plot is time domain, lower trace is frequency domain plot for 25 seconds worth of data.

Figure 8 shows the background microphonics when the cryogenic piping was undergoing a thermoacoustic oscillation. The data in the upper plot is the time domain data from an accelerometer which was placed on a plate that is attached to the valve stem of the JT valve. The second plot shows the resultant microphonics which exceeded the requirements by a factor of ten. The third plot shows the frequency domain plot of the microphonics and accelerometer signals. It should be noted that although the 90 Hz and 120 Hz valve vibrations were about an order of magnitude larger than the 46 Hz components, the resultant microphonics at 46 Hz was 10 times larger than any other

Content from this work may be used under the terms of the CC BY 3.0 licence (© 2019). Any distribution of this work must maintain attribution to the author(s), title of the work, publisher, and DOI.

harmonic. This was due to the amplification effect that the modal resonance at 46 Hz which is shown in Fig. 2.

Figure 8 shows the effect of JT valve operation on the microphonics. When the JT valve was operated it caused a 120 Hz vibration that was primarily transverse to the beam line direction. It also produces a vibration nearly an order of magnitude smaller at 30Hz, 40 Hz and 80 Hz. Again, these modes are amplified by modal resonances at 45 Hz and 80 Hz in the structure that are shown in Fig. 3.

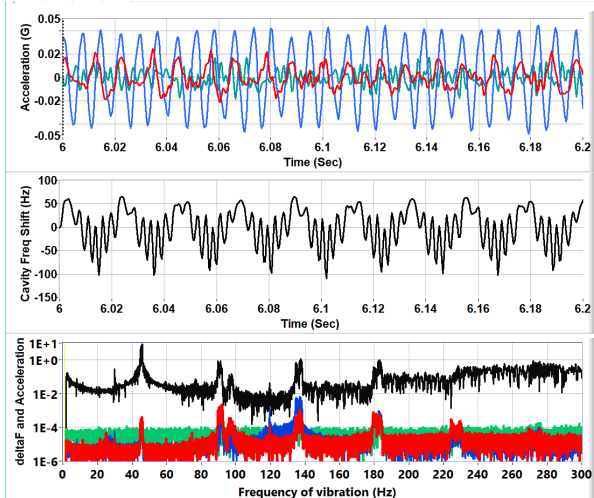


Figure 8: Prototype cryomodule cavity 7 readings from an acceleration of the JT valve (red, blue and green) and background microphonics (black) and when the cryogenics where in a state of thermoacoustic oscillation.

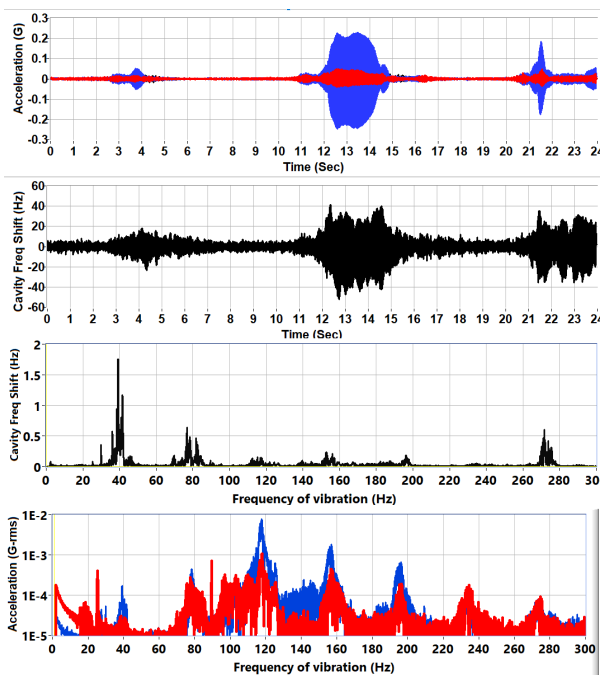


Figure 9: Prototype cryomodule cavity 7 background microphonics and accelerometer readings while the JT valve was being operated.

In Fig. 9, the valve control loop implemented a 0.6% change in position, and there was a large microphonics transient. Figure 10 shows the effect JT-valve operation

had on the microphonics in cryomodule CM10. The short, smaller microphonics bursts shown in Fig. 10 is more typical of the later cryomodules. In this instance the first two pulses were position changes of 1% and the third is a 2% change in position. One hypothesis is that the additional wipers on the JT-valve actuator shaft couple it to the tube and dampen the vibrations of the actuator shaft. No effort was made to optimize the JT-valve control algorithm in order to reduce these vibrations. Figure 11 shows the background microphonics for CM10 with no JT valve motion.

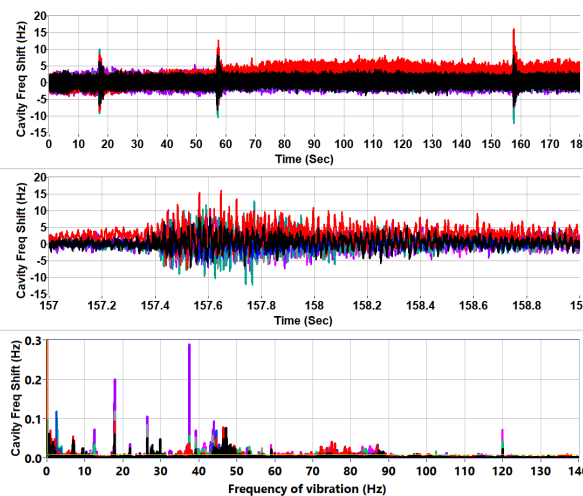


Figure 10: Typical transient which occurred when the JT-valve was actuated. CM10 cavities 1, 2, 4, 5, 6, 7, and 8.

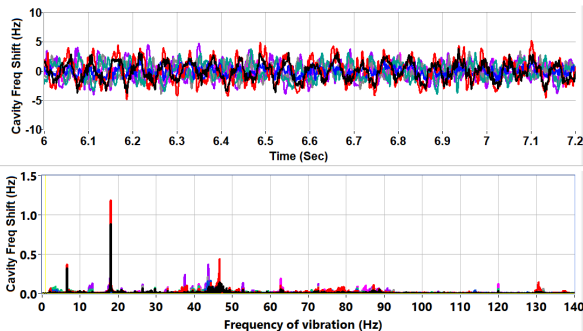


Figure 11: Background microphonics for cavities 1, 2, 4, 5, 6, 7 and 8 of CM10. Data taken simultaneously.

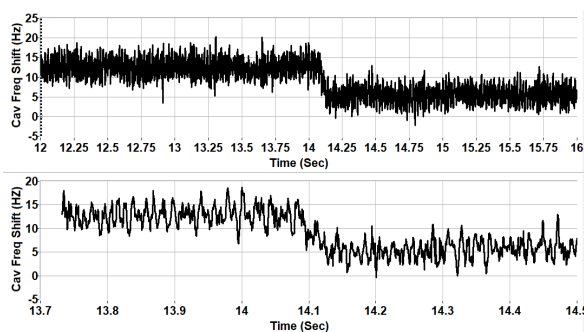


Figure 12: Measured microphonics when the tuner motor is operated in a full step mode.

One of the other concerns when designing a cryomodule is whether operation of the tuner induces added

microphonics when the stepper motor is operated. Figure 12 shows the effect of operating a single tuner motor and changing the cavity resonant frequency by 10 Hz. There was no indication of excess microphonics when the motor was operated.

### Comparison of Background Microphonics and Transfer Function

Figure 13(a) shows a comparison of the background microphonics and the transfer function for the cavity pCM-1. Figure 13(b) shows the same data for CM10-1. Similarly, Fig. 14 shows the results for cavities pCM-5 and CM10-5 respectively. In Fig. 13(a) and 14(a) the modes at 42 Hz and 29.8 Hz, respectively, are much larger than the vertical scale, which was reduced in order to allow one to see the other narrow band modes. A significant contributor to 29.8 Hz mode in the prototype cryomodule was that the mounting plates were not properly bolted to the concrete floor which allowed them to vibrate vertically. Even with proper mounting plate installation two of the tests (not shown in this work) had significant 29.8 Hz, 59.7 Hz, 89.6 Hz, and 149.3 Hz vibrations. The most likely cause of these vibrations was a nearby motor with a failing bearing.

The changes in the cryomodule design between the prototype and CM10 shifted the mode at 10 Hz down to 7 Hz where it became susceptible to some form of background vibration. 7 Hz is a known vibration frequency of the chilled water tower which is located about 25 m from the cryomodule. The design changes and improved cryomodule mounting in the test cave also reduced the Q of or moved the frequency of the 30 Hz modal resonance in CM10, which made it less sensitive to that source of excitation. Cavity 5 continued to have a 46 Hz modal resonance which was not excited as much in CM10 as the 42 Hz was in the prototype cryomodule.

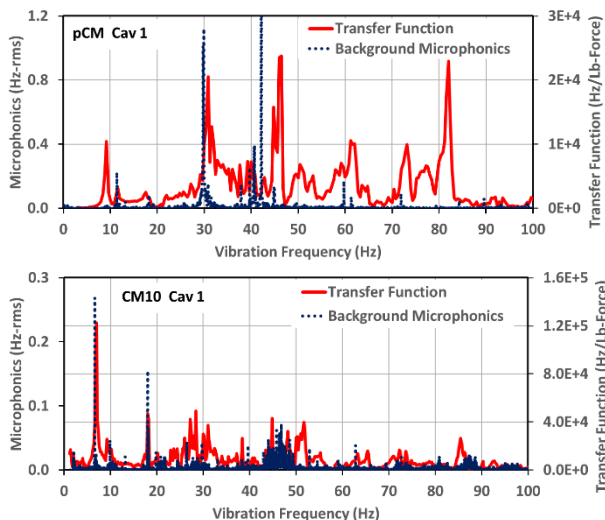


Figure 13: Transfer function as compared to the background microphonics for (a) cavity 1 on the prototype cryomodule and (b) cavity 1 on CM10.

In all of these results one can observe that the narrow band microphonics noise frequently overlapped with

modal resonances. This generally indicates a mode which is driven by a narrowband external source. The broadband noise, such as is seen in CM10 between 45 and 55 Hz, is typical for a modal resonance driven by broad band noise. It should be noted that the cryogenic piping and the floor of the test facility were sources of several narrowband vibrational excitations with narrow vibrational lines every few Hertz up to a few hundred Hertz.

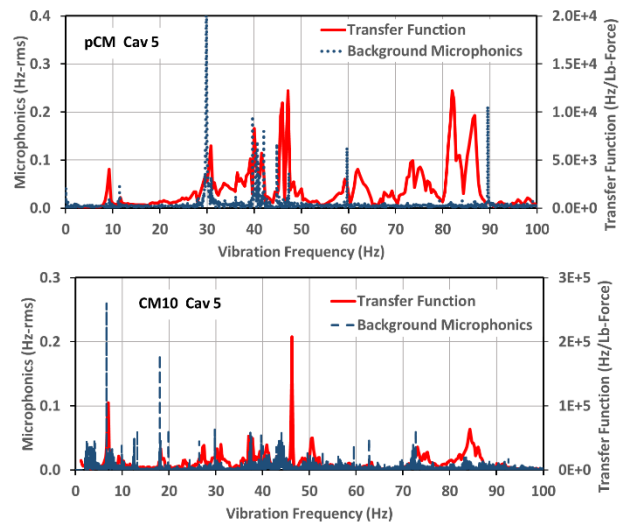


Figure 14: Transfer function as compared to the background microphonics for (a) cavity 5 on the prototype cryomodule and (b) cavity 5 on CM10.

## SUMMARY

The prototype cryomodule had excessive microphonics with the dominant cause being thermos-acoustic oscillations in the helium supply piping. There were a number of issues relating to the installation in the test cave and the cryogenics system design. The cryogenic design issues were dominated by a thermoacoustic oscillation in the JT valves. Both the cryogenics and installation issues were addressed on subsequent cryomodules. Subsequent cryomodules generally met the 10 Hz peak microphonics spec for steady state operations. However, operation of the JT-Valve in the JLab cryomodule test cave produced vibrations which caused the cavities regularly exceed 14 Hz peak microphonics and occasionally exceeded 18 Hz. These value would exceed the available RF power when the cavities are operated at 16 MV/m and at full beam loading and no beam loading respectively. These tests were carried out in the JLab cryomodule test facility which has different background vibrations than the tunnel will have at LCLS II. Modal analysis and the use of accelerometers to measure vibrations of external components are useful tools for understanding and mitigating microphonics issues.

## REFERENCES

- [1] J.R. Delayen. "Phase and amplitude stabilization of superconducting resonators", Ph.D. Thesis, Caltech, 1978
- [2] T. Plawski, G. K. Davis, H. Dong, C. Hovater, J. Musson, and T. Powers, "Digital Cavity Resonance Monitor - Alternative Method of Measuring Cavity Microphonics", in *Proc. 12th*

*Int. Conf. RF Superconductivity (SRF'05)*, Ithaca, NY, USA, Jul. 2005, paper THP63, pp. 616-618.

- [3] Z. Gao, H. Yuan, C. Chang, T. Powers, "A new microphonics measurement method for superconducting RF cavities", *Nucl. Instrum. Methods Phys. Res., Sect. A*, 767, 212–217, Nov. 2014.
- [4] G. K. Davis, J. Matalевич, T. Powers, and M. Wiseman, "Vibration Response Testing of the CEBAF 12 GeV Upgrade Cryomodules", in *Proc. 26th Linear Accelerator Conf. (LINAC'12)*, Tel Aviv, Israel, Sep. 2012, paper MOPB031, pp. 240-242.
- [5] G. Wu, E. Harms, "LCLS II Prototype Cryomodule Testing", presented at TTC workshop, Feb. 2017, Madison, WI, USA.

Content from this work may be used under the terms of the CC BY 3.0 licence (© 2019). Any distribution of this work must maintain attribution to the author(s), title of the work, publisher, and DOI.